HIGH PRESSURE SPARK GAP RECOVERY AFTER OVERVOLTED BREAKDOWN

Stuart Moran and Shelton Hairfield

Naval Surface Weapons Center
Dahlgren, VA 22448

Abstract

A spark gap at pressures from 100 kPa to 7 MPa with various gases is fired by overvolting the electodes. The recovery of the gap is studied using a second identical pulse to test the voltage holdoff during the recovery period. A TV camera, interferometer and a spinning mirror camera are also used to record arc locations and density profiles. The gas is stationary during the recovery. Breakdown voltages go up to 130 kV, currents are hundreds of amps and voltage risetimes are about 1 kV/ nsec. Results show the effects of gas species, electrode material and pressure on both breakdown voltages and recovery curves. The recovery of the ability to be overvolted occurs much slower than the recovery to DC breakdown voltages. The effects of the first arc on the second arc locations are shown as well as density profiles using a Mach-Zender interferometer.

Introduction

High pressure spark gap switches are well suited for high powers, fast turn-on, and low impedance; but have difficulty operating at high repetition rates. The energy lost in the switch is deposited in a small region which must return to normal before the gap can recover. Although high-power blowers can physically remove the energy by removing the hot gas, they deprive the spark gap switch of its small size and high efficiency. It is therefore very desirable to improve the inherent recovery mechanisms of the switch itself. This work studies the factors that limit the recovery of a spark gap in which the gas is stationary. A two-phase technique is used to measure the recovery of a gap subjected to a fast rising pulse that overvolts the switch. Video cameras and an intererometer are used to study the location of the arcs and the density profiles of the disturbed region.

Experimental Setup

The spark gaps used in these experiments are untriggered, solid, cylindrical Rowgowski-shaped electrodes made of brass, elkonite or graphite and range in diameter from 20mm to 70mm. They are used in open air, or housings made from plexiglass or epoxy. See Figure 1. The housings have quartz optical windows and can withstand pressure up to 7 MPa. Gap spacing is adjusted by a micrometer and can be varied from .1mm to 5mm. The gas can be exchanged slowly (lml/sec) to prevent long term changes due to by-products. The gases used in these experimants are dry air, hydrogen, helium, and argon.

A diagram of the two-pulse circuit is shown in Figure 2. The 20.8 nF capacitors are charged to 30kV. When one of the thyratrons is triggered, it dumps its capacitor through the 5:1 step-up transformer to produce a voltage pulse across the spark gap. The voltage rises at a rate of about 1kV/nsec with an approximately linear ramp up to a maximum of 140 kV. After a preset time delay, The second thyratron is triggered to produce a second identical pulse which is used to indicate the recovery of the spark gap. Since all of the energy initially stored in the spark gap is discharged through the gap, the amount of energy going through the gap is constant regardless of the breakdown voltage. A series resistor is used to limit the current through the thyratrons, and to damp the circuit. The current through the gap peaks at a few hundred amps and lasts for about a half a microsecond. A resistive divider and a current viewing resistor provide the voltage and current signals.

The fast-rising voltage ramp causes the statistically varying time to breakdown to produce a variation in breakdown voltage. A transient digitizer system is used to obtain means and standard deviations of the data. The static breakdown voltage is measured with a high-voltage D.C. supply.

Video cameras and still cameras are used to observe the location of the arc channels on the electrode surface.

To obtain density profiles during the recovery period, a Mach-Zender interferometer is used with a spinning-mirror framing camera. See Figure 3. The interferometer uses a helium-neon laser to produce a 4 cm interference pattern through the windows of the spark gap. The pattern is recorded on 35mm film using a Beckman-Whitley framing camera. The mirror spin rate provides a 3 microsecond exposure time and 8 microseconds between each of 25 frames. The camera can record up to 2 milliseconds after the spark without rewrite. To measure the interference patterns for time periods greater than a millisecond, high-speed Fastax moving-film cameras were used at 5,000 frames/second.

Experimental Results

Breakdown Voltage

The breakdown voltage of a spark gap under a ramp voltage pulse is determined by both the static breakdown voltage, which is a function of the pressure-spacing product, and the amount of overvoltage, which is a function of the rate of rise of the voltage pulse and the time for the formation of the spark channel. Our experiments show that while pulsed breakdown is a linear function of gap spacing, it is not a linear function of gas pressure.[1] The percent of overvoltage is greater at atmospheric pressures than at higher pressures. Results show that varying the electrode material has a significant effect on the amount of overvoltage. For our fast rising pulses, elkonite showes the most overvoltage, graphite the least.

Recovery Curves

Figure 4 shows an example of the percent recovery as a function of time. Percent recovery is the ratio of the average second pulse breakdown to the average first pulse breakdown for a particular time delay. Thirty samples were taken for each data point. The standard deviation for both the first and second pulses ranged from 2 to 20 percent. The recovery curves for all of the gases, electrodes, and spacings tested generally have a plateau or inflection point that occurs near the static breakdown voltage for the particular set of parameters. The explanation for this appears to be that the recovery of an overvolted gap occurs in two stages. The first stage is the recovery of a voltage corresponding to the static breakdown voltage. This occurs on the order of a few milliseconds. The second stage is the recovery of the ability to be overvolted and occurs over a much longer time frame, often greater than a second. Therefore, for an overvolted gap, complete recovery will occur only after the ability to be overvolted is reacquired. Since this is a very slow process, overvolting a spark gap may drastically reduce its maximum repetition rate. While the electrode material, gas pressure and gas species affect the significance of the second stage, the major factor controlling the time necessary for the second stage to recover is the gap spacing. The recovery time is directly proportional to gap spacing.[2]

Spark Location

Open shutter photographs and video recordings show that generally the second spark does not follow the path of the first spark, even when the gap has only recovered a few

Report Documentation Page	*Form Approved* *OMB No. 0704-0188*

1. REPORT DATE	2. REPORT TYPE	3. DATES COVERED
JUN 1985	**N/A**	**-**

4. TITLE AND SUBTITLE	
High Pressure Spark Gap Recovery After Overvolted Breakdown	5a. CONTRACT NUMBER
	5b. GRANT NUMBER
	5c. PROGRAM ELEMENT NUMBER
6. AUTHOR(S)	5d. PROJECT NUMBER
	5e. TASK NUMBER
	5f. WORK UNIT NUMBER
7. PERFORMING ORGANIZATION NAME(S) AND ADDRESS(ES) **Naval Surface Weapons Center Dahlgren, VA 22448**	8. PERFORMING ORGANIZATION REPORT NUMBER
9. SPONSORING/MONITORING AGENCY NAME(S) AND ADDRESS(ES)	10. SPONSOR/MONITOR'S ACRONYM(S)
	11. SPONSOR/MONITOR'S REPORT NUMBER(S)

12. DISTRIBUTION/AVAILABILITY STATEMENT

Approved for public release, distribution unlimited

13. SUPPLEMENTARY NOTES

See also ADM002371. 2013 IEEE Pulsed Power Conference, Digest of Technical Papers 1976-2013, and Abstracts of the 2013 IEEE International Conference on Plasma Science. Held in San Francisco, CA on 16-21 June 2013. U.S. Government or Federal Purpose Rights License.

14. ABSTRACT

A spark gap at pressures from 100 kPa to 7 MPa with various gases is fired by overvolting the electodes. The recovery of the gap is studied using a second identical pulse to test the voltage holdoff during the recovery period. A TV camera, interferometer and a spinning mirror camera are also used to record arc locations and density profiles. The gas is stationary during the recovery. Breakdown voltages go up to 130 kV, currents are hundreds of amps and voltage risetimes are about 1 kV/ nsec. Results show the effects of gas species, electrode material and pressure on both breakdown voltages and recovery curves. The recovery of the ability to be overvolted occurs much slower than the recovery to DC breakdown voltages. The effects of the first arc on the second arc locations are shown as well as density profiles using a Mach-Zender interferometer.

15. SUBJECT TERMS

16. SECURITY CLASSIFICATION OF:			17. LIMITATION OF ABSTRACT	18. NUMBER OF PAGES	19a. NAME OF RESPONSIBLE PERSON
a REPORT **unclassified**	b ABSTRACT **unclassified**	c THIS PAGE **unclassified**	**SAR**	**4**	

Standard Form 298 (Rev. 8-98)
Prescribed by ANSI Std Z39-18

percent of its breakdown voltage. This was true of all gases and presures. The second sparks occur in a cylindrical region around the first spark and this region expands with time. This indicates that the weakest point of the interelectrode region is not necessarily the original breakdown channel. It also indicates that a hot electrode spot at the center of the initial spark does not control recovery.

Figure 5 shows how the distance from the first spark to the second varies with time for air at atmospheric pressure. Each curve represents about 1000 shots and the resolution is about 1mm. The housing was removed to prevent shock wave reflections. The sparks are confined to a cylindrical region (the direction is random) which expands until the gap has recovered its static holdoff voltage at about 50 milliseconds. At this point the region is about one cm in diameter. At later times, the second spark locations become more random and approach the independent distribution by the time the second stage of recovery is complete. The luminous spark channel, as recorded by video cameras, has a diameter of about one mm for high pressures and a few mm for atmospheric pressures.

Interference Patterns

Figure 6A shows an interference pattern before the spark fires. The top electrode goes across the whole pattern while the bottom electrode is smaller to localize the spark within the interference pattern and the optical windows. The interference lines are not straight due to poor surfaces on the cube beamsplitters. Gap spacing is 0.5 cm. Some light from the arc (which is defocused) appears in Figure 6A. Figure 6B shows the pattern in air at atmospheric pressure 8 microseconds later. A downward deflection in the lines indicates a decrease in number density of the gas. After 8 microseconds a shock wave leaves this low density region and propagates away. The shock velocity drops from about Mach 2 in Figure 6C to Mach 1.3 in Figure 6D as it propagates out of the field of view. No reflections from the housing can be seen. A discountinuity behind the shock wave can be seen in Figures 6C and 6D. However, the 3 microsecond exposure time blurs the shock front and makes it difficult to follow the fringe lines through it. The low density region centered around the spark expands quickly to about 0.5 cm in diameter (in 10 microseconds) and then remains fairly constant out to hundreds of microseconds, when the fringe lines begin to swirl indicating turbulent convection (Figure 7A and 7B). Once turbulence starts, density profiles are difficult to obtain.

Figure 8A and 8B show a breakdown in helium at 617 kPa (75 psig). The size of the low density region is about the same as for air but the shock wave travels faster due to the higher sound speed. Shock wave velocities are about Mach 1.3. Figure 8C shows Helium one millisecond after the spark. Note that there is very little turbulence. The data showed that for all of the gases, the onset of turbulence occurs more rapidly as the gas pressure is increased. Turbulence occurred within 10 microseconds in air or hydrogen above a few atmospheres. However for atomospheric pressure hydrogen and for helium up to several atmospheres, turbulence did not occur for at least a millisecond. Lack of turbulence makes a mathematical description of recovery much simpler. Figure 8D shows a second spark breakdown occurring one millisecond after the first. Shock wave velocities for the second pulses, even for very little recovery, had about the same velocity as the first.

Figure 9A shows hydrogen at 617 kPa (75 psig) one millisecond after firing a spark which occurred near the left edge of the lower electrode. After the gas becomes turbulent the remains of the turbulent gas localize near the upper electrode. Figures 9B, C, D show the second arc. The second arc does not go through the location of the luminous channel of the first arc but does originate in the remants of the first arc. The first spark breakdown voltage was 120 kV and the second was 50 kV. The spark remnants in Figure 9A appear to have risen due to bouyancy forces but calculations showed that the bouyancy forces are too slow. Figure 10A and 10B shows a spark firing horizontally. Figure 10C shows that after a millisecond the remnants still go toward the large electrode. Figure 10D shows the second spark going through the remnants. Polarity, and electrode tips were changed and it was concluded that current direction, polarity and the external circuit were not factors. It appears to be the effects of electrode geometry on the mass flow into the low density region. A similar situation occurs in air but on a much slower time scale.

Figure 11 shows the effects of varying the energy dumped through the gap in air at atmospheric pressure. Figure 11A and 11B are with 3.0 nF stored on the primary capacitors and Figure 11C and 11D are with 20.8 nF, a factor of seven. With higher capacitance the low density region is about twice the volume indicating more energy is dissipated in the gas. The shock wave velocities and the onset of turbulance are almost the same for both cases.

The high speed moving film cameras show that the density profiles return to the normal background after a few milliseconds in hydrogen and a few tens of milliseconds in air. The heated regions continue to expand slowly during the later time period out to a diameter of about two cm. This corresponds closely to the arc locations in Figure 5.

Conclusions

For a fast rising pulse, the amount of overvoltage depends on gap spacing, electrode material and gas pressure. For a given charging waveform, increasing the gas pressure reduces the amount of overvoltage. Recovery of an overvolted gap occurs in two stages. The first is the recovery of gas density, which will provide the gas with its static holdoff voltage. This typically occurs in a few milliseconds and is independent of electrode material. The second stage is the recovery of the ability to be overvolted. This is a slow process and depends strongly on the gap spacing. Recovery of this stage can require seconds for gaps larger than a few millimeters. The mechanism for this slow recovery has not been determined.

The spark column heats a cylindrical region of gas which expands to orders of magnitude larger volume than the luminous channel. Most of this expansion occurs in the first 10 microseconds. If a second voltage pulse is applied to this region. The spark channel will form within this large heated region but not necessarily through the original spark channel.

The expanding gas forms a shock wave which separates from the heated region after about 10 microseconds and propagates away at slightly supersonic speeds.

The onset of turbulence can be controlled by gas density and species. For currents of a few hundred amps, hydrogen and helium are non-turbulent at atmospheric pressures. This simplifies modeling problems. Increasing gas pressure speeds up the onset of turbulence. Air or hydrogen above several atmospheres becomes turbulent within 10 microseconds.

Electrode geometry plays an important role in determining the gas dynamics and where the gas remnants collect.

Increasing the amount of energy dumped through the gap increases the size of the disturbed region. However, the shock wave velocities and the onset of turbulence remain the same.

References

1. S. Moran and S. Hairfield, "Recovery of Overvolted Spark Gaps," 16th Power Modulator Symposium, Washington, D.C., June 18-20, 1984.

2. S. Moran and S. Hairfield, "Recovery of Overvolted Spark Gaps," 16th Power Modulator Symposium, Washington, D.C., June 18-20, 1984

Acknowledgement

The authors would like to thank Marilyn Schwellenbach for her help in setting up the optics.

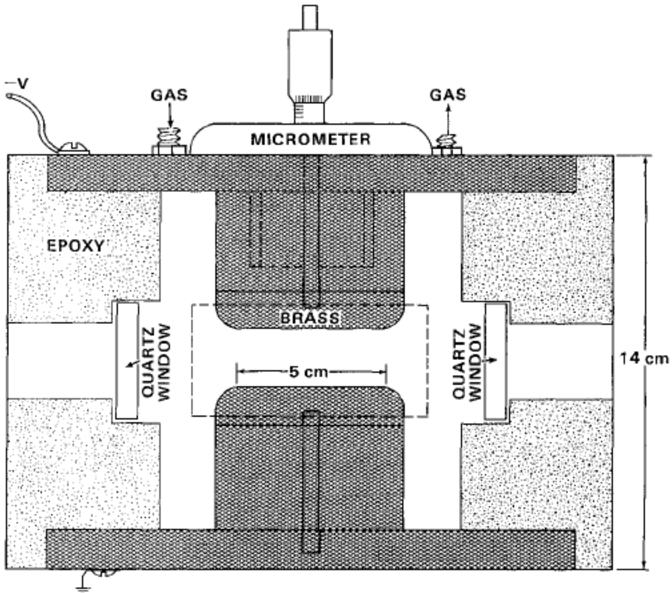

Fig. 1. Spark gap housing

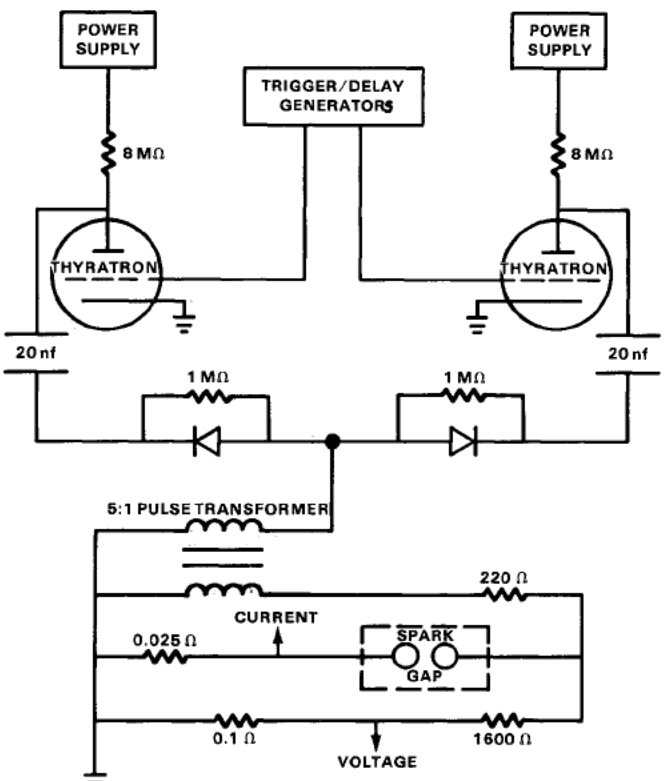

Fig. 2. Two-pulse circuit

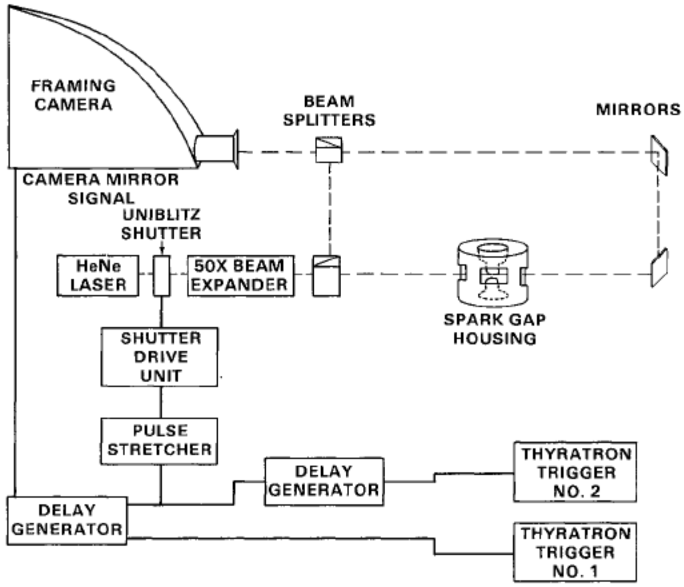

Fig. 3. Interferometer and camera setup

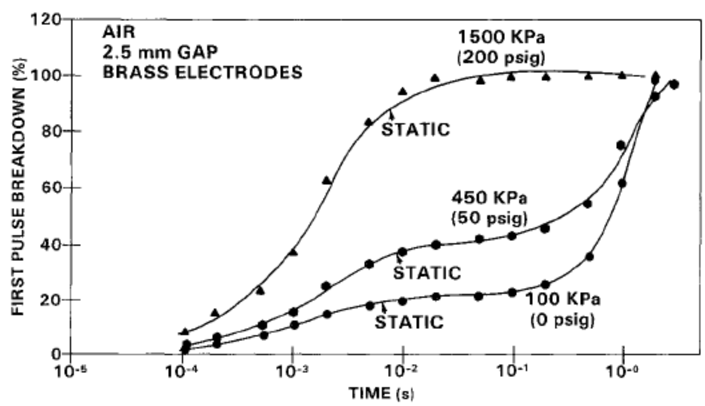

Fig. 4. Recovery of air

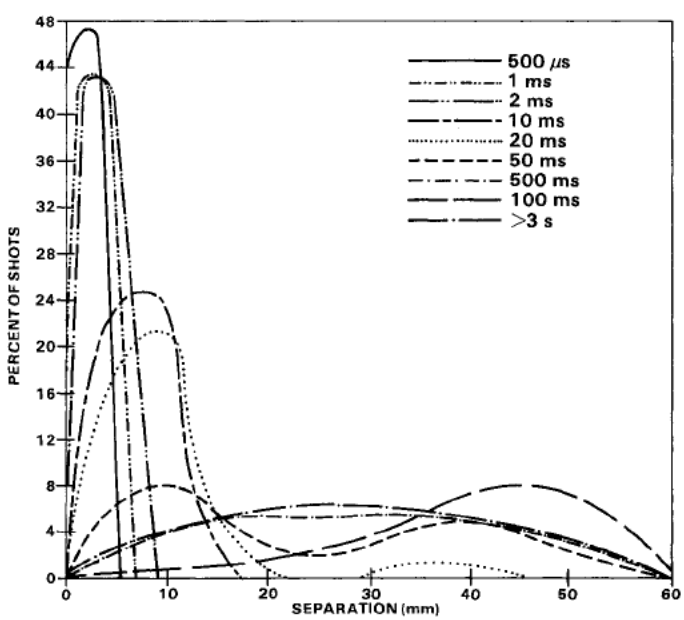

Fig. 5. Spark separation in atmospheric air

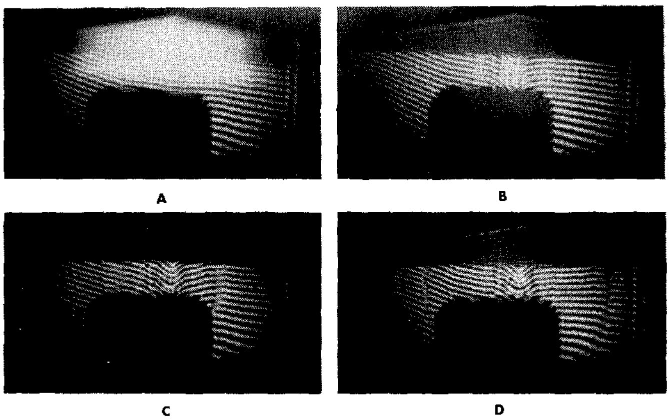

Fig. 6. Interferograms of breakdown in air at atmospheric pressure. Time after spark:
A - 0 μ sec B - 8 μ sec C - 16 μ sec D - 32 μ sec

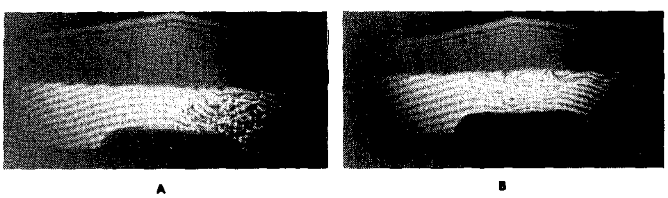

Fig. 7. Turbulance in air at atmospheric pressure.
Time after spark: A - 467 μ sec B - 2.18 millisec

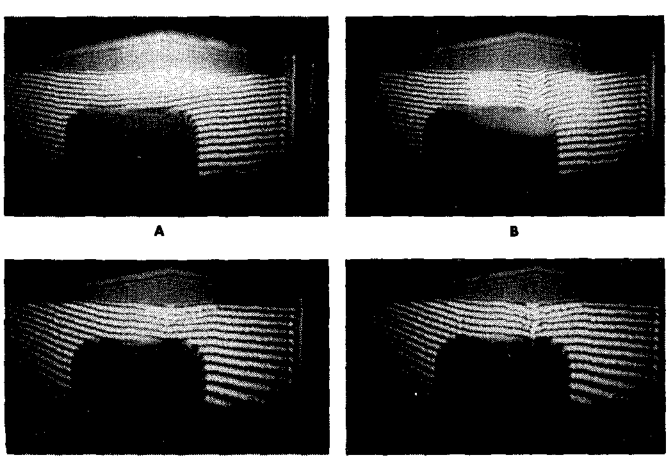

Fig. 8. Helium at 617 kPa (75 psig)

A - Background pattern B - 8 μ sec after breakdown
C - 1.2 millisec after breakdown
D - 1.1 millisec after first spark,
8 μ sec after second spark.

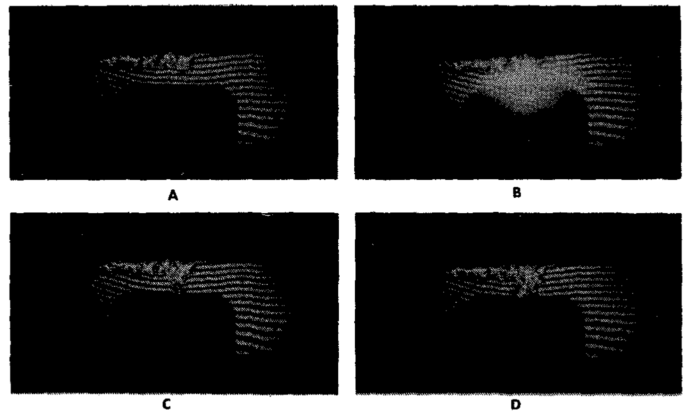

Fig. 9. Hydrogen 617 KPa (75 psig)

A - 1.1 millisec after spark B. second spark starting
C - 8 μ sec after second spark D - 80 μ sec after second spark

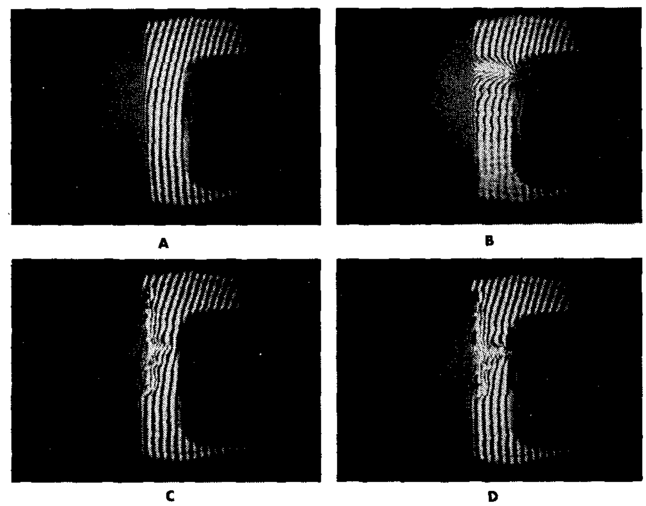

Fig. 10. Hydrogen 450 kPa (50 psig), gap turned on its side.

A - before breakdown B - 8 μ sec after first spark
C - 1.1 millisec after first spark D - 8 μ sec after second spark

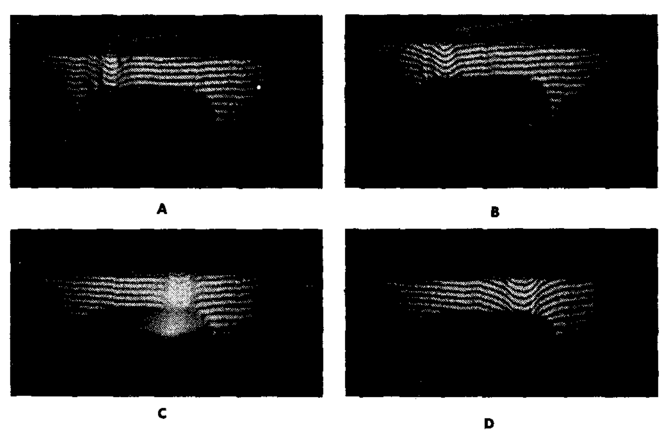

Fig. 11. Air at atmospheric pressure, energy varied.
Capacitance and time after breakdown:

A - 3.0 nF, 8 μ sec B - 3.0 nF, 16 μ sec

C - 20.8 nF, 8 μ sec D - 20.8 nF, 16 μ sec